Methylamine Gas Based Synthesis and Healing Process Toward Upscaling of Perovskite Solar Cells: Progress and Perspective

Chongwen Li, Shuping Pang, Hongxia Xu, and Guanglei Cui**

Perovskite solar cells (PSCs) have aroused a wide range of interests in recent years due to their high power conversion efficiency. Traditional fabrication methods of perovskite layer such as one step spin coating, two step deposition and vapor deposition have been comprehensively studied for laboratory preparation. In this progress report, a rapidly developing methylamine (MA) gas based method is reviewed, which enables the large scale fabrication of high quality perovskite layer and extends the possibility of PSCs application in industrial preparation. The MA gas based method is related to solid-gas reactions, and the mechanisms of those special transformation processes of different solid-gas systems are discussed. Finally, a perspective of this promising PSCs fabrication method is given. However, as this method was only developed for a few years, there remain some unexplored areas for further investigation.

1. Introduction

Organic-inorganic metal halide perovskites (OIMHPs) are a series of ABX_3-structured materials, in which B and X are respectively inorganic ions Pb^{2+}, Sn^{2+} and halogen ions I^-, Br^-, or Cl^-, etc.[1] The perovskite structure is constructed by corner sharing BX_6 octahedrons, with A site organic cations such as $CH_3NH_3^+$ (MA^+) or $NH=HCNH_3^+$ (FA^+) restricted in it by the help of electrostatic force. As feedback, the size of organic groups also acts crucially for the formation of one dimensional (1D) to three dimensional (3D) crystal structures.[2–6] The essence is the value of the tolerance factor t, which could be calculated based on their ionic radius following the formula of (where r_A, r_B, and r_X are the ionic radii of A, B, and X, respectively). So far, only the organic MA^+ and FA^+ satisfy the requirement of t between 0.8 and 1 which enable the forming of 3D perovskite structure.[4,7,8] Benefiting from their unique structural characteristics, the OIMHPs have outstanding properties of wider and stronger optical absorption, lower trap density, proper carrier diffusion length and better defect tolerance than traditional photoelectric materials, which make them extremely attractive for solar cell devices and other modern device applications.[9–14] Another advantage of the OIMHPs is their solution processing feasibility, but it is unfortunately always accompanied by some intrinsic drawbacks. The rough and multi-defect perovskite film fabricated from precursor solution will inevitably damage the device performance.[15] Although some strategies, such as sequential dipping, two-step spin-coating, and anti-solvent methods, along with recently developed atmosphere (solvent such as N,N-dimethylformamide and dimethyl sulfoxide, or methylamine chloride) assisted methods, could improve the quality of perovskite layer, there still exist drawbacks when we assess their potential for further practical applications which require both scale enlargement and time-efficiency improvement.[16–20] Thus a more cost-effective, time-saving and easy-operating preparation method is imperative.

As shown in **Figure 1**, many traditional technologies have been preliminarily tried to fabricate high quality perovskite films with large scale, such as roll-to-roll method, doctor blading process, spray coating, inkjet printing, slot-die printing, etc.[21–23] The perovskite solar cell modules are also fabricated and studied, but the efficiency and reproducibility of them are relatively poor compared with the devices with small working area.[22,24] The key problem is the difficulty in controlling the perovskite films quality with a large scale, which in turn highly degrades the module performance. Very recently, a methylamine (MA) gas induced defect-healing method was developed to improve $MAPbI_3$ film quality and enhance the performance of perovskite solar cells (PSCs).[25] This MA gas method seems more promising compared to the traditional PSC fabrication methods, as it requires low demand for precursor film quality and can be completed in very short period of time, which make it quite attractive for commercial production. Generally, this MA gas method can be described as the reaction between organic MA gas (or FA gas) and perovskite solid ($MAPbI_3$ and $FAPbI_3$). Taking the typical $MAPbI_3$ as example, once the $MAPbI_3$ perovskite solid exposures to MA gas, the solid material starts to fade and liquefy. This transformation usually happens in a very short timescale (few seconds). After the removal of MA gas atmosphere, the liquefied intermediate phase returns to its

C. Li, Dr. S.Pang, Dr. H. Xu, Dr. G. Cui
Qingdao Industrial Energy Storage Technology Institute, Qingdao Institute of Bioenergy and Bioprocess Technology, Chinese Academy of Sciences, Qingdao 266101, P.R. China
E-mail: pangsp@qibebt.ac.cn; cuigl@qibebt.ac.cn

DOI: 10.1002/solr.201700076

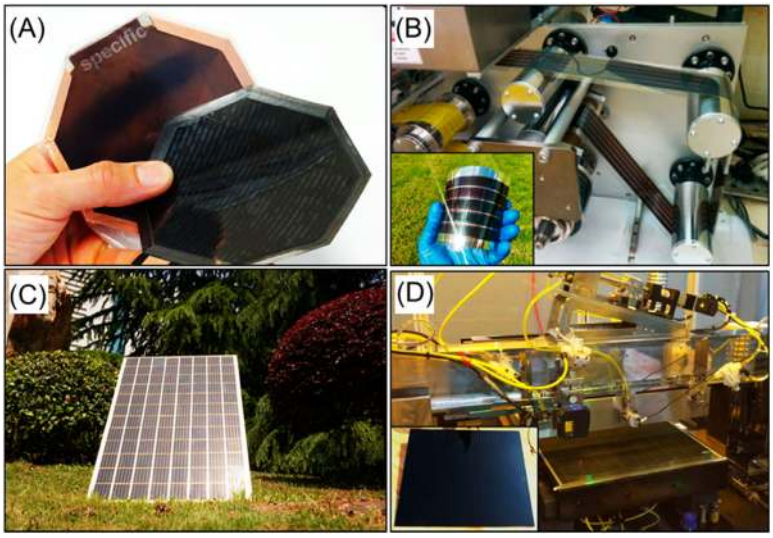

Figure 1. (A) Printed PSC on low-cost metal foil. (B) Roll-to-roll fabrication of MAPbI3 perovskite thin films based on slot-die coating process. The inset shows a printed flexible module. (C) Carbon-based hole-conductor-free mesoscopic PSC modules. (D) Slot-die coating fabrication of perovskite thin film on a rigid substrate. Reproduced with permission.[21] Copyright 2016, American Chemical Society.

original black brown color and turns out to be with much better film quality. So far, there are numerous outstanding works been reported based on this special gas-solid chemistry reaction for optimizing perovskite films, and the mechanism understanding becomes more and more crucial for more precise modification of film morphology, crystal property and further large scale process optimization as well.[26–30]

Herein, we review this innovative perovskite film modification method which could tremendously enhance perovskite film quality and promote the development of the large scale fabrication for PSC devices. The reaction chemistry is expounded here for better understanding of this special reaction, while some unknown aspects of it are reasonably assumed with according evidences. Numerous works concentrated on different gas-solid reaction systems are classified and described here. Finally, we give our outlook about this MA gas based method and hope it will be more intensively and extensively investigated by more groups to make progress of it.

2. The Structural Transformation

Perovskite thin films fabricated by simple one-step spin-coating method are usually with poor morphology. This may arouse from the heterogeneous growth of the perovskite or its intermediate crystals during the evaporating of the solvents. Upon the complete conversion to perovskite crystals, the film morphology is figurate with large amounts of pin-hole defects. Up to now, many methods have been developed to synthesis or healing the perovskite films based on the organic MA gas, such as PbI_2-MA, $HPbI_3$-MA, NH_4PbI_3-MA, and $MAPbI_3$-MA, etc. (**Figure 2**(A)–(D)), where the PbI_6 octahedron framework can be reconstructed to turn the film with a better morphology. To better understand the transformation process of the reaction, it is necessary to investigate the role of each component in the perovskite lattice. Pristine PbI_2 at room temperature adopts 2H polytype, and it is a typical hexagonal layered-structure material which is connected by weak interlayer van der Waals interactions between adjacent layers (Figure 2(A)).[31–34] Previous works found that various electron-donating molecules (such as nitrogen-containing molecules R-NH_3) can intercalate into the interlayer of PbI_2 and change its coordination geometry.[35–37] More specifically, the nitrogen-containing molecules will insert into the spaces which are connected by van der waals forces, thus PbI_2 layers will slide to form a more stable configuration.[38] The reason was considered as the proximal bonds formed by the strong Pb-N interaction between Pb^{2-} from PbI_2 layer and the closest N atom from $-NH_3$.[39,40] However, some experiments found that other metal and organic iodides such as KI, CsI, MAI could also react with the MA to form a liquid phase. That hints that the hydrogen bond may be non-negligible in this process.[41,42]

For the purpose of figuring out whether the B-site metal ions and X-site halogen make difference, $MAPbBr_3$ and $MASnI_3$ samples are set by Jen et al. to react with MA gas in the same condition.[43] The very similar transformation phenomenon of them indicates that these two aspects are not the determinant. Further when the organic component is changed, which is $FAPbI_3$ or $CsPbI_3$, there exhibits a different performance when exposing to MA gas. The $FAPbI_3$ film fades and becomes smoother while $CsPbI_3$ exhibits no change in color but an obvious change in morphology.[41] The difference strongly suggests the significance of the hydrogen bond effect in determining the readiness of the reaction between MA gas and perovskite.

The intermediate phase in the transformation process is vital for the mechanism understanding, however although there are some XRD patterns and UV–Vis measurements, it still remains unknown what the exactly structure is of it. Hitherto, the only determinate thing is that PbI_6 octahedrons in the intermediate liquid phase are transformed to low dimensional structures, while the degassing process is accompanied by the reconstruction of 3D perovskite structure. During this reconstruction process, the recovery of 3D perovskite structure also facilitates the removal of MA molecules. Very recently it was found that Cs-MA-mixed perovskite films also can react with MA gas. The difference is that the containing A-site Cs^+ could obviously accelerate MA degassing speed which therefore promotes the rapid recovering of 3D perovskite structure. This is because Cs^+ doping can reduce PbI_6 octahedron distortion, which in turn enhances the electrostatic interaction in the perovskite structure. The improved electrostatic interaction also provides the positive effect on the improved moisture stability.

When tracing the formation process of perovskite by two-step soaking method, it is found that the organic ammonium iodide

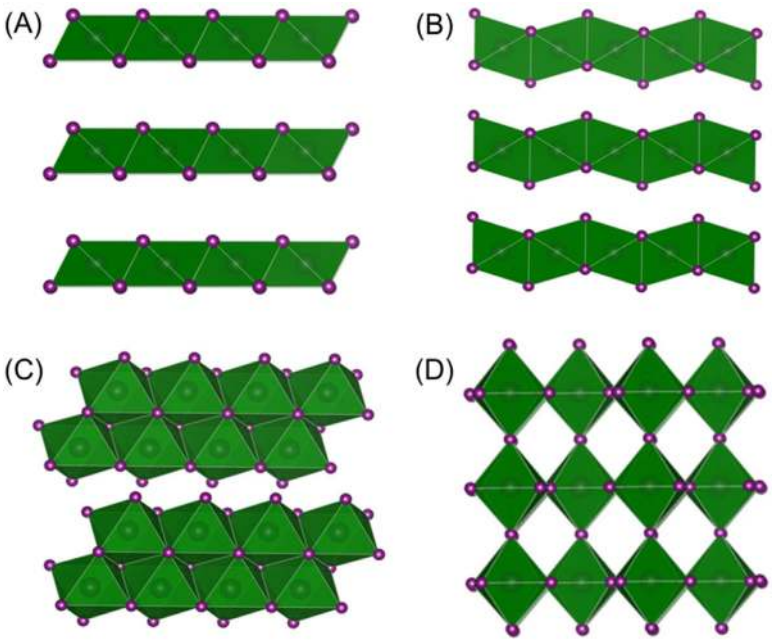

Figure 2. The PbI_6 octahedron framework in layered hexagonal PbI_2 (A, edge sharing), one dimensional $HPbI_3$, or δ-$FAPbI_3$ (B, face sharing), one dimensional NH_4PbI_3 (C, face sharing) and three dimensional $MAPbI_3$ or α-$FAPbI_3$ perovskite phase (D, corner sharing).

(such as R-NH_3I) can react with layered PbI_2 in solution, in the form of breaking Pb-I bonds by the I^- from foreign organic groups.[44,45] The hydrogen bonds between $-NH_3$ and the nearest I^- will be formed, helping the insertion of organic group to the interstices of PbI_6 octahedrons. The opened PbI_2 structure will then be rearranged, transforming the edge-sharing structure to corner-sharing (both in-layer and between layers), thus the 3D PbI_6 octahedron is built. It is worth noting that when dipping PbI_2 solid film into MAI solution, each layer of the opened PbI_2 are surrounded by MA^+ in the solution before the remove of excess MAI.[39] This indicates that with excess MA^+ in the compound, Pb-I structure tends to form a loose layered structure sandwiched by MA cation.

Based on the evidences above, it is proposed that when treating $MAPbI_3$ with MA gas, the excess MA molecule will insert into the PbI_6 octahedron of perovskite and thus expand the interstices between them. In this stage, the hydrogen bonds between foreign MA molecules and I^{2-} in PbI_6 are considered as the main drive force for the gas up-taking reaction. When the amount of the inserted MA molecules surpasses the tolerance of PbI_6 framework, the structure may be further opened. Withal, the $-NH_3$ of foreign MA molecule could build partial Pb-N bonds, making the PbI_6 octahedron distorted. Due to the nature of the weak bond and the thermodynamics tendency of the 3D perovskite structure recovery, the MA gas will spontaneously degassed once the liquid is removed away from the MA gas atmosphere. That is to say, the MA gas up taking and degassing processes are the rearrangement processes of the PbI_6 octahedron, which therefore induce the changes of the color, morphology and crystallinity.

3. Homogeneous Organic Cation Gas-Solid Process

The homogeneous organic cation gas-solid process mainly refers to the reactions between MA gas and $MAPbI_3$ perovskite. The typical experiment process could be carried out as follows. The pristine $MAPbI_3$ thin film is beforehand prepared by simple spin-coating and annealing. Then the raw film is put a few centimeters above the methylamine alcohol solution (**Figure 3**(A)), reagent mixture of KOH and MACl powders (Figure 3(B)) or in the chamber which is full of organic MA gas with preferred pressure (Figure 3 (C)). When contacting MA gas, the black perovskite film turns to transparent immediately. After that the sample is removed from the atmosphere, and then it subsequently restores to its original black brown color with very smooth appearance.[25] Besides the direct contact between $MAPbI_3$ perovskite solid and MA gas, the MA source can also be introduced dissolving in solvent (Figure 3(D)).[46]

As mentioned in plenty of works, the pristine $MAPbI_3$ films usually reveal very poor coverage and morphology. PSCs fabricated by this kind of uneven perovskite layer are normally with low performance due to the high recombination rate at the multi-defects areas. When the pristine perovskite film exposes to MA gas, a transformation happens from black brown solid $MAPbI_3$ perovskite to transparent liquid intermediate $MAPbI_3 \cdot xMA$ phase (Eq. (1-1)). This transformation usually completes in seconds. Upon the releasing of MA gas, the value of x in the intermediate phase decreases resulting in the supersaturation of $MAPbI_3$ in the intermediate phase. The supersaturation drives $MAPbI_3$ to recrystallize and returns back to its origin black brown color but with much smoother morphology (Eq. (1-2)).[25,43,47–49] The mechanism is vividly illustrated by the in situ experiment on the transformation of two black faceted $MAPbI_3$ perovskite crystals in/out MA gas monitored by microscope, which is shown in **Figure 4**(A).

$$CH_3NH_3PbI_3(s) + xCH_3NH_2(g) \rightarrow CH_3NH_3PbI_3 \cdot CH_3NH_2(l) \quad (1\text{-}1)$$

$$CH_3NH_3PbI_3 \cdot CH_3NH_2(l) \rightarrow CH_3NH_3PbI_3(s) + xCH_3NH_2(g) \quad (1\text{-}2)$$

Analyzing from the above observation, two important points should be concluded here. The first is that the solid to liquid transformation process is reversible for perovskite as the blacken and solidification happens upon the remove of MA gas (Figure 4 (A)). This proves the possibility of MA gas treatment for perovskite. The second is the liquefied intermediate compound is flowable (Figure 4(B)).[50] This enables the even spreading of perovskite intermediate phase on substrate which can cover the defects such as pinholes and the infiltration of it to mesoscopic layer which improve the contact area between these two layer. However direct evidence such as the morphology of the intermediate phase is hard to detect by the use of traditional SEM or TEM measurement due to its instability. As a result, the morphology of the MA gas treated $MAPbI_3$ perovskite film is

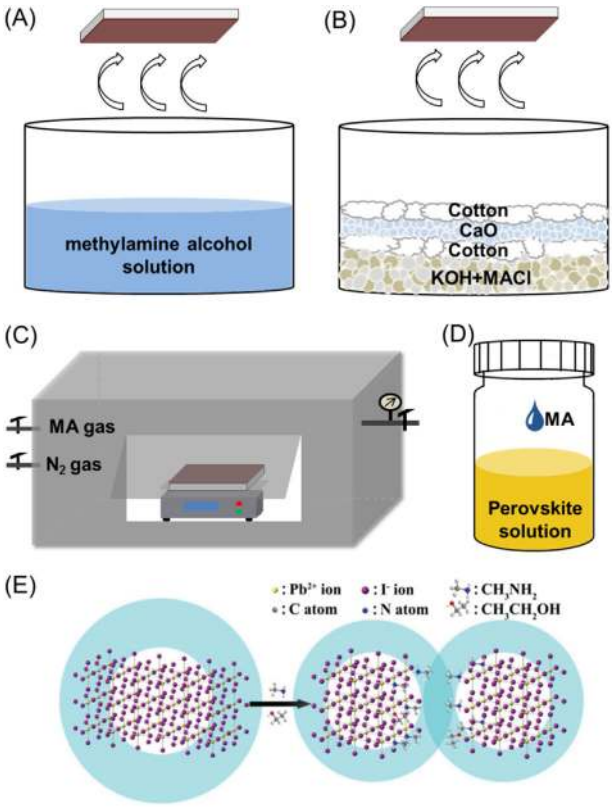

Figure 3. Different MA gas based methods to fabrication highly uniform perovskite films. (A) The MA gas is from the methylamine alcohol solution. (B) The MA gas is from the mixture of KOH and MACl powders. (C) A chamber which can be used to control the atmosphere and gas pressure. (D) MA molecules are induced in precursor solution. (E) The schematic illustration of the particle size evolution in the solvent induced after the MA molecules introduction. Reproduced with permission.[46] Copyright 2017, Wiley-VCH.

better covered than the pristine film as can be seen in Figure 4(C) and (D), while the crystal size seems slight smaller after the treatment.

The property of perovskite grain boundaries is another important factor to determine the quality of perovskite films.[27,51] As reported before, perovskite grain boundaries are usually where with a large density of charge traps. These will act as recombination centers promoting the non-radiation recombination of carriers, which further reduces the carrier separation. To increase the grain size and quality can to some extend diminish this negative effect. However, the MA gas treatment induced change in crystal size is not that positive (Figure 4(C) and (D)). But the XRD peak intensity of the MA gas treated sample is extremely enhanced which means that the perovskite film is highly orientated with (110) crystal plane (Figure 4(E)). The higher crystallinity of the treated perovskite can effectively reduce the defects and thus improves the device performance, with the efficiency increased from 5 to 15%. This may be related to its intermediate structure of $MAPbI_3 \cdot xMA$ and the recrystallization process, but it is still unclear now. The decrease in crystal size is a common result of the MA gas treated perovskite film and it may induce some potential undesirable effects for PSC devices both in photoelectric conversion efficiency and the stability. In this case, Zang et al. in their work employ a thermally induced recrystallization of $MAPbI_3$ during the liquidation process to enhance grain size.[49] By setting the solid $MAPbI_3$ perovskite film under MA gas atmosphere at elevated temperature, the expulsion of MA molecules in $MAPbI_3 \cdot xMA$ is controlled which regulates the supersaturation of the intermediate system and the perovskite recrystallization rate. The average grains size in this work grows up to about 15 μm. However, its photoelectric property are still not studied and it seems that such a large grain is hardly possible to be a single crystal structure, which has been discussed in other similar systems.[52–54] The $MAPbI_3 \cdot xMA$ intermediate phase is concluded to play an important role in the transformation process. However, due to its transiency and instability, the measuring of this phase remains difficult. To put the perovskite thin film in a low concentration MA gas atmosphere can keep the transparent intermediate phase longer. The characteristic diffraction peak of ~7.2° is found from XRD measurement of the long-lived intermediate $MAPbI_3 \cdot xMA$, which suggests the swelling of $MAPbI_3$ lattice. But detailed information of the structure is still lack.[43] The other common results of the MA gas treated perovskite film are the slight increase of the band gap and the decrease of the photoluminescence (PL) intensity.[43,51] One possible reason may be the formation of the MA-rich perovskite layer with excess MA molecules in the perovskite structure, but it still needs to be further determined.

Derived from this $MAPbI_3$-MA reaction, a series of new methods have been developed to synthesis perovskite films. Zhao et al. develop a one-step method using PbI_2, HI acid, and MA gas as reactants.[48] In their work, the precursor film is prepared from the solution of equal molar HI acid and PbI_2 in N, N′-Dimethylformamide (DMF) solvent and the film is spin-coated under MA gas atmosphere. The MA molecules can diffuse into the precursor films during spin coating. After that, annealing is adopted to remove extra solvent and excess MA molecules. Finally, pure phase perovskite is obtained and the PSC devices fabricated by this method are comparable to the devices which are from traditional MAI precursor. The reaction mechanism of the reaction ($PbI_2 + HI + MA(g) = MAPbI_3$) is discussed as first-step constructing of $HI \cdot PbI_2$ structure which is very similar to $MAPbI_3$ in solution. Then in the spin process, MA gas molecules can intercalate into $HI \cdot PbI_2$ lattice forming $MAPbI_3$ perovskite.

Qi et al. employs the similar system of $PbI_2 + MA(g) + HI$ to synthesis $MAPbI_3$ in ambient atmosphere.[28] In his method, PbI_2 film is firstly spin-coated on the substrate followed by an annealing treatment. Then the PbI_2 film is exposed to MA gas and HI gas either sequentially or simultaneously to transfer into $MAPbI_3$. Lead oxide (PbO_x) and $Pb(OH)_2$ are generated as byproducts by the help of H_2O in ambient atmosphere as shown in Eq. (2-1) to Eq. (2-3). These byproducts will be further iodinated into PbI_2 under HI acid atmosphere (Eq. (2-4) and Eq. (2-5)). As shown in **Figure 5**, in this work when using MA gas to treat PbX_2 (X = I, Br, and Cl respectively), the perovskite formation time increases from that for $MAPbCl_3$ to $MAPbI_3$ which should be related with the stronger interaction between iodine-based methylamine salt and methylamine molecules. This highly supports the vital role of hydrogen bonds between

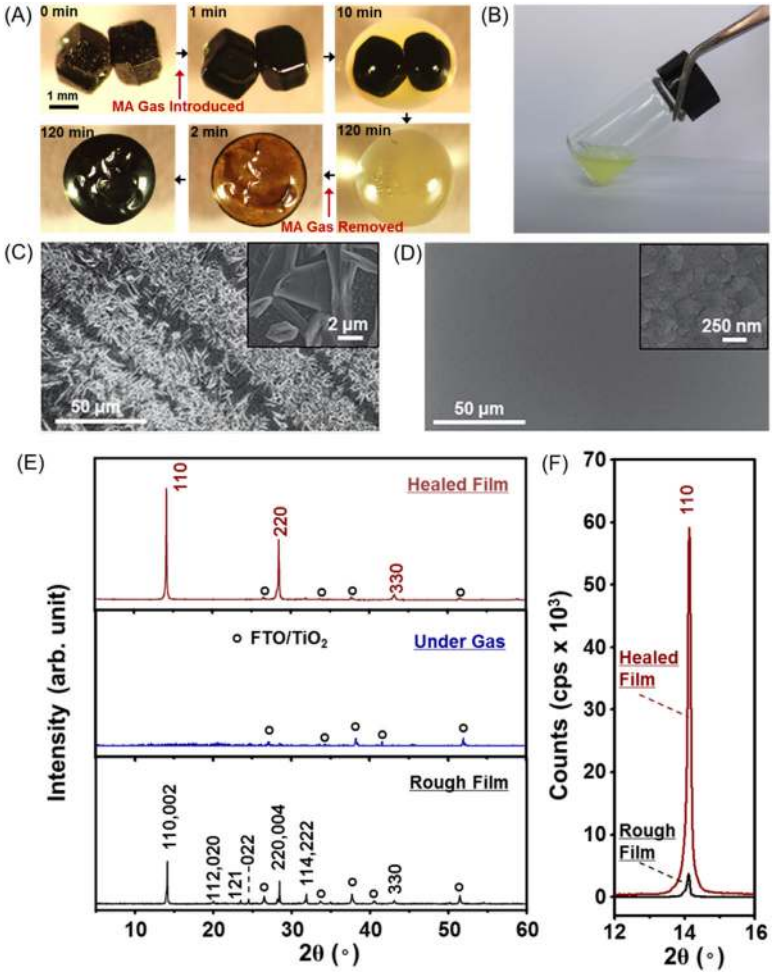

Figure 4. (A) In situ optical microscopy of the morphology evolution process of two adjacent $MAPbI_3$ perovskite crystals upon MA gas exposure/degassing. (B) Liquefied $MAPbI_3$ under MA atmosphere. (C) SEM images of pristine $MAPbI_3$ film morphology and (D) MA gas treated $MAPbI_3$ film morphology. (E) XRD patterns of the perovskite thin film at origin state, under MA gas atmosphere and after gas treating. (F) XRD patterns of the (110) face of raw and treated $MAPbI_3$ perovskite films. (A), (C)–(F) are reproduced with permission.[25] Copyright 2015, Wiley-VCH.

foreign MA molecules and the halogen PbX_6 for the MA gas treating reaction.

$$3PbI_2 + 2CH_3NH_2 + H_2O \rightarrow 2CH_3NH_3PbI_3 + PbO \quad (2\text{-}1)$$

$$CH_3NH_2 + H_2O \rightarrow CH_3NH_3OH \quad (2\text{-}2)$$

$$3PbI_2 + 2CH_3NH_3OH \rightarrow 2CH_3NH_3PbI_3 + Pb(OH)_2 \quad (2\text{-}3)$$

$$PbO + 2HI \rightarrow PbI_2 + H_2O \quad (2\text{-}4)$$

$$Pb(OH)_2 + 2HI \rightarrow PbI_2 + 2H_2O \quad (2\text{-}5)$$

The generation of PbO_x and $Pb(OH)_2$ can also help the formation of luminescent $MAPbBr_3$ perovskite films. Zhao et al. in their work employs MA gas to react with $PbBr_2$ in ambient atmosphere to fabricated $MAPbBr_3$ perovskite films with high luminescent property.[55] In this work, the intermediate products of PbO_x and $Pb(OH)_2$ can act as frameworks which confine the grain growth of $MAPbBr_3$ crystals and localize the quantum confinement effect.

As mentioned above, the grain boundaries of perovskite play a negative role in the device performance. Qi et al. introduce MA gas to the annealing step to eliminate grain boundaries and gaps.[47] In this work, MAPbI3 pristine film is spin-coated using anti-solvent method. Then the film is annealing on a heating plate in MA gas atmosphere. It is found that the simultaneous MA gas exposure and solvent evaporation in the annealing process can greatly improves the diffusion of MA molecules during the perovskite formation, which contributes to the film uniformity. Moreover, MA gas intercalation in the elevating temperature will be accelerated according to the Arrhenius equation. As a result, the impurities at grain boundaries are largely reduced and the intra-layer carrier recombination induced both by the defects of grain boundaries and through grain gaps are effectively eliminated.

It hass been reported that excess PbI_2 in annealed perovskite film can help passivate perovskite, but the dosage of PbI_2 needs to be properly controlled.[56] Zhao et al. develop a precisely controllable MA gas assisted reaction to fabricated PbI_2 passivated $MAPbI_3$ films.[57] In this work, perovskite films are fabricated from hydro-halide deficient $PbI_2 \cdot xHI$/Br precursor solutions by adding different amount of HI/Br acid in the solutions. The perovskite film fabricated from the deficient stoichiometric precursor solutions remains different amount of excess PbI_2 in the final annealed films, which is beneficial for the PSC devices.

In MAPbI3 precursor solutions, I^- is prone to oxidize to I_2, which will inevitable introduce trap states in the final thin films. Zhou et al. in their work found that by adding methylamine alcohol solution in the precursor solution, the oxidization of I^- is eliminated due to the disproportionation under alkaline condition aroused by excess MA molecules dissolved in the system. The eliminating process can be described as Eq. (3-1).

$$3I_2 + 6CH_3NH_2 + 3H_2O \rightarrow 5I^- + IO_3^- + 6CH_3NH_3^+ \quad (3\text{-}1)$$

Besides, in $MAPbI_3$ precursor solutions, the excess foreign MA molecules are suggested to coordinate to Pb (II) center competing with other ligands such as I^- and DMF. This can trim the large particles in the precursor solutions to small pieces, in which the mechanism is very similar to that of dimethylsulfoxide (DMSO) case in previous work (Figure 3(E)). With the partially substituted iodoplumbate by MA or ethanol, the concentration of

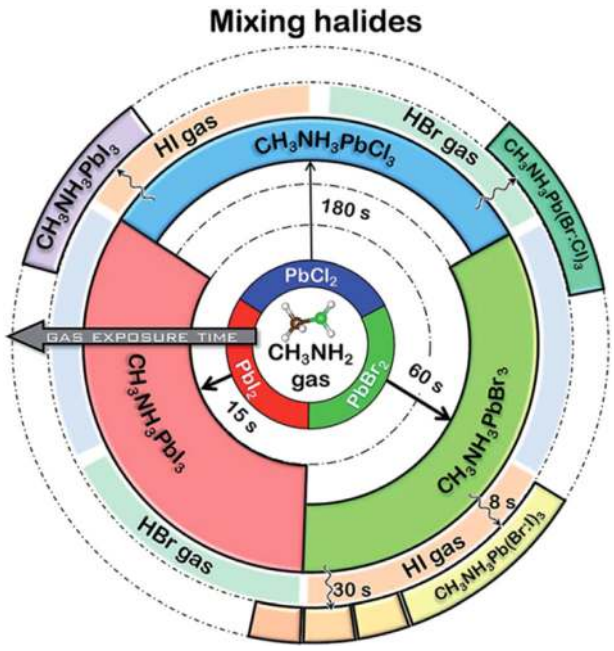

Figure 5. The conversion process between PbX_2 (X = I, Br, and Cl) films, MA gas and HI/HBr gases. It represents all the possibilities of lead halide exposures to MA and hydrogen halide gases. After the initial conversion of PbX_2 to $CH_3NH_3PbX_3 + PbO/Pb(OH)_2$ upon MA gas exposure, the perovskite can be finely tuned to mixed-halide perovskite, by converting $PbO/Pb(OH)_2$ to PbI_2 or $PbBr_2$ after HI or HBr gas exposures, respectively. The reactions happen at different time-scales depending on the halide: I (15 s) < Br (60 s) < Cl (180 s). Chlorine is not favorable to form uniformly mixed-halide perovskite, but only phase-segregated perovskites. [Original citation] — Published by The Royal Society of Chemistry.[28]

polyiodide complexes are decreased, which reduces the defects of perovskite.

Snaith et al. in their work demonstrate an alternative strategy to introduce MA gas by employing acetonitrile (ACN) to be the solvent of precursor solution.[26] The solubility of PbI_2 in ACN is highly increased after bubbling MA gas in the solution and pale yellow perovskite solution is thus gained. The $MAPbI_3$ tetragonal perovskite in this method is very easy to form even before the annealing process, and high quality, super smooth perovskite film is fabricated after slight annealing to evaporate the remaining solvent. Apart from the seeking of high PCE, the possibility of large scale fabrication by this method is also a critical issue which improves the feasibility of further application.

The industrial preparation process such slot-die coating is promising for PSCs fabrication. On the basis of MA gas-solid reaction mechanism, Zhou et al. have fabricated flexible $MAPbI_3$ perovskite cell on polyethylene terephthalate (PET) substrate by using slot-die coating method, and the area of the MA gas modified perovskite film is enlarged to several square centimeters.[25] However, when concerning the solution process, the possibility is highly decreased on account of the restricted selection of solvent such as DMF, DMSO, and γ-butyrolactone (GBL). The MA gas assisted perovskite salt dissolution strategy provides us a broad selection when choosing proper solvents for large scale fabrication.[26,46]

4. Heterogeneous Gas-Solid Process

Heterogeneous gas-solid process is the reaction between nitrogen-containing gas (MA, FA, NH_3) and the ABX_3 material, in which the A site component is different from the gas.

NH_3 is a kind of smaller amine molecule compared to MA, and it causes a relatively slow color change compared to $MAPbI_3$-MA reaction when reacting with MA gas (**Figure 6**(A)). The transparent intermediate phase will then return to black after the removal of MA gas atmosphere.[59–61] The intermediate phase is analyzed by XRD measurement which shows characteristic peaks at lower degree compared to $MAPbI_3$ perovskite. This indicates the expansion of the lattice. However, the specific value of this peak varies in different works.[27,30,59–61] This may be related to the different NH_3 gas pressure and measurement temperature in these works, which influence the intermediate phase's component. So due to the intermediate phase's instability, the structure identification still needs further investigation. It has been known that $MAPbI_3$ perovskite shows high absorption intensity ranging from ~780 to 400 nm in visible light spectrum, while the NH_3 gas treated film absorbs shows no absorption signal in this region. This rapid-changed and contrast absorption property in a wide spectral range makes it possible to fabricate NH_3 sensor using $MAPbI_3$ perovskite.[60] Another significant change by NH_3 gas treatment is the resistance between $MAPbI_3$ and the intermediate phase. The pristine $MAPbI_3$ film normally shows high resistance, and once melted and faded by NH_3 gas, the resistance of the intermediate phase decreases rapidly. This shows that in the current test set up in the form of sharply increase of current intensity. After removing NH_3 gas, the current density returns to low correspondingly. The rapid resistance response of the transformation process makes it promising to fabricate NH_3 sensor with fast response time.[61] It has been reported that the longer exposure time can destroy the reversibility of the color change of $MAPbI_3$ with/without NH_3 gas atmosphere, but the limited time varies from tens of seconds to tens of minutes in different works.[59–61] The uncertainty of exact composition of the treated material and the transformation reversibility limited time may be determined by the specific experimental condition which varies in different works.

As ABX_3 structured material, NH_4PbI_3 adopts one-dimensional structure due to its relatively low value of tolerance factor (Figure 2(C)). By exposing the light yellow NH_4PbI_3 crystal in MA gas atmosphere, the rod like structure gradually turns to black and then starts to collapse and fade. The intermediate phase spreads smoothly on the substrate during the treatment and returns back to black brown after the removal of MA gas.[30] Unlike what is observed in the case of MA-$MAPbI_3$ system, an additional step of NH_4PbI_3 blackening happens before turning to liquid phase.[25] The transformation process can be divided into two sequential reactions Eq. (4-1) and Eq. (4-2).

$$NH_4PbI_3(s) + MA(g) \rightarrow NH_3(g) + MAPbI_3(s) \quad (4\text{-}1)$$

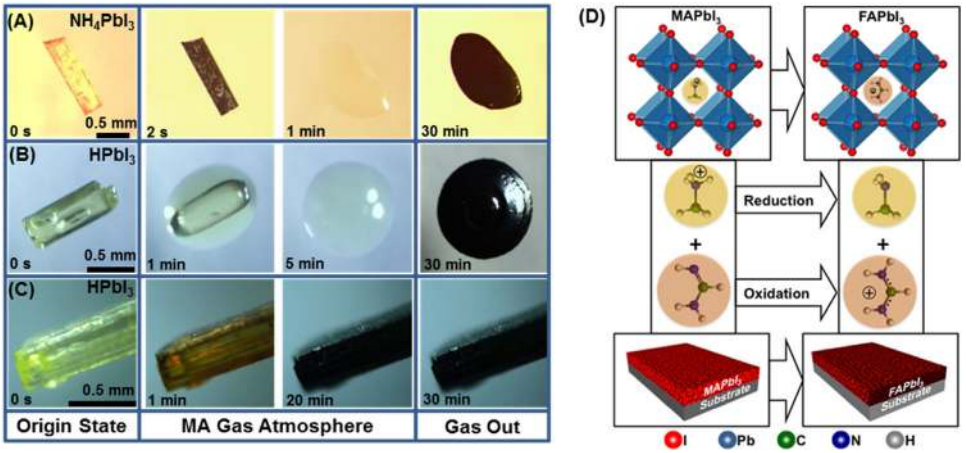

Figure 6. (A) In situ optical microscope observation of the transformation from NH_4PbI_3 to $MAPbI_3$ induced by MA gas at room temperature. Reproduced with permission.[27] Copyright 2016, Wiley-VCH. In situ optical microscope observation of the transformation from $HPbI_3$ to $MAPbI_3$ induced by MA gas at (B) room temperature and (C) 150 °C. Reproduced with permission.[58] Copyright 2016, American Chemical Society. (D) Cation displacement reaction between $MAPbI_3$ perovskite and FA gas at 150 °C. Reproduced with permission.[29] Copyright 2016, American Chemical Society.

$$MAPbI_3(s) + xMA(g) \rightarrow MAPbI_3 \cdot xMA(l) \rightarrow MAPbI_3(s) + xMA(g) \quad (4\text{-}2)$$

In Eq. (4-1), the nitrogen bonded hydrogen atom of MA^+ is trapped by ammonia molecule. In Eq. (4-2) step, the reaction is very similar to that of MA-MAPbI3 process. When putting NH_4PbI_3 polycrystalline thin film in MA gas atmosphere, the small crystals on the substrate also go through the same conversion process as the large crystal, and the special blacken and morphology preserved phenomenon of small NH_4PbI_3 crystals is further detected by PL maps on top the film.[30] It has been reported that when putting NH_4PbI_3 thin film in MA gas atmosphere, the thin film can convert to $MAPbI_3$ more rapidly than the reaction between $MAPbI_3$ and NH_3 gas. This is explained by the density functional theory (DFT) calculation, which shows proper activation energy and enthalpy change for proton transfer from NH_4^+ to MA molecule.

$FAPbI_3$ perovskite is considered to be promising because of its proper band gap and higher thermal stability compared to $MAPbI_3$ perovskite.[7,62] There are two polymorphism of $FAPbI_3$ in ambient atmosphere, which are trigonal α-$FAPbI_3$ black phase and hexagonal δ-$FAPbI_3$ yellow non-perovskite. For these two $FAPbI_3$ polymorphisms, yellow non-perovskite phase is more stable than black phase at room temperature. Unfortunately, when $FAPbI_3$ film is exposed to MA or FA gas, yellow color film is obtained.[43] The XRD pattern indicates that it is with a structure similar to hexagonal δ-$FAPbI_3$ non-perovskite phase.[29] In this case, the molecule or ion exchange method is therefore reasonable because it can preserve the perovskite structure and prevent the direct formation of undesired yellow phase. Padture et al. introduce a FA gas-solid reaction for the fabrication of $FAPbI_3$ perovskite follows the reaction of $MAPbI_3(s) + FA(g) \rightarrow FAPbI_3(s) + MA(g)$ in FA gas atmosphere at elevated temperature as shown in Figure 6(D).[29] This transformation process can be considered as protonation reaction from FA to FA^+ and deprotonation reaction of MA to MA^+. After the full conversion, α-$FAPbI_3$ phase is tightly fixed and the δ-$FAPbI_3$ is effectively avoided. This may be a result of the more stable α-$FAPbI_3$ perovskite state at high reaction temperature. What should be note is that the $FAPbI_3$ film morphology is highly preserved.

Another promising precursor reactant for MA gas assisted fabrication is $HPbI_3$. In the room temperature conversion process, $HPbI_3$ crystal turns to transparent liquid phase upon contacting MA gas and returns back brown to black $MAPbI_3$ after the removing of MA gas.[58] This process proceeding under room temperature is shown in Figure 6(B). The mechanism is described as the first reaction (Eq. (5-1)) of $HPbI_3$ and MA gas which forms $MAPbI_3$, and the as-formed $MAPbI_3$ will then further react with MA gas which is very similar to the MA-$MAPbI_3$ system (Eq. (5-2)).

$$HPbI_3(s) + CH_2NH_2(g) \rightarrow MAPbI_3(s) \quad (5\text{-}1)$$

$$HPbI_3(s) + (1+x)CH_3NH_2(g) \rightarrow MAPbI_3 \cdot xCH_3NH_2(l) \rightarrow MAPbI_3(s) + CH_3NH_2(g) \quad (5\text{-}2)$$

The role of H^+ in $HPbI_3$ is very crucial in this process as it is provided as the acid part of the strong acid-base interaction between H^+ and MA gas. Besides, the already formed Pb-I bonds in $HPbI_3$ enables a near-topotactic conversion of $HPbI_3$ structure to $MAPbI_3$ perovskite structure. The morphology of $MAPbI_3$ film transferred by this process is ultra-smooth and the performance of the fabricated PSC device is thus improved. In the high temperature condition as shown in Figure 6(C), the liquidation seems not to occur. This is because in the high temperature, reaction 5-2 is not preferred to happen.

Yan et al. in their work add MA ethanol solution in $HI + PbI_2$ precursor solution to fabricate high quality and highly stable perovskite thin film.[63] The reaction process is illustrated in **Figure 7**. In precursor solution, HI will coordinate to Pb (II) forming face-sharing PbI_6 octahedral linear columns, and

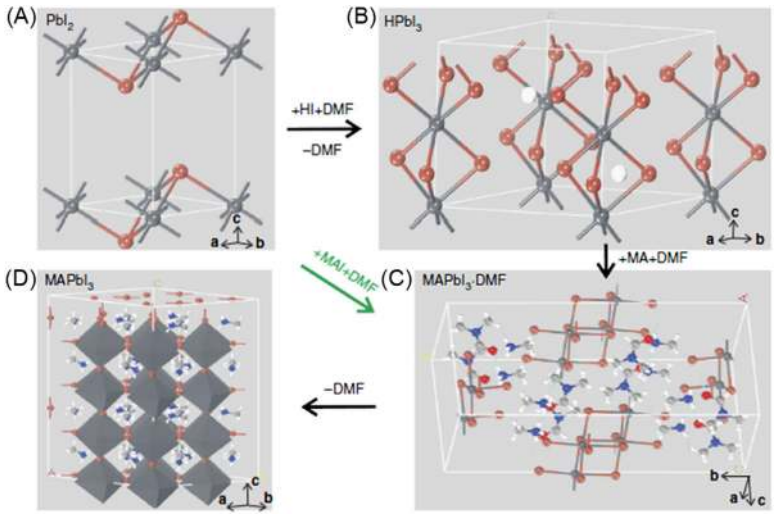

Figure 7. Crystallographic illustration of the conversion from PbI_2 to $HPbI_3$, then to intermediate $MAPbI_3 \cdot DMF$, finally to $MAPbI_3$. Reproduced with permission.[63] Copyright 2016, Nature Publishing Group.

simultaneously turns to $HPbI_3$ hexagonal array upon the intercalation of DMF (Figure 7(A) and (B)). Upon the adding of MA ethanol solution, MA molecule is inserted in between $HPbI_3$ structure (Figure 7(C)). After the removal of DMF solution, the $[PbI_3]^-$ chain will be opened and thus the tetragonal perovskite structure is formed (Figure 7(D)). While in the case of stoichiometric MAI/PbI_2 system, DMF plays a competitor role which influences the full iodine coordination for stoichiometric perovskite.[64] As a result of the full coordination and stoichiometry by this method, the perovskite film quality and stability are strongly enhanced.

5. Perspectives and Challenges

We here have summarized the emergence of the gas-solid method for the fabrication and modification of OIMHPs films. The organic gases (MA and FA) primarily act as the organic reactant or the initiator gas of the transformation process. The solid (pristine film)-liquid (intermediate phase)-solid process (final film) enhances the performance of perovskite film in two aspects. One is the perovskite morphology, including film coverage, roughness, and the compactness of perovskite-adjacent interlayer; The other one is the grain quality, including grain orientation and grain boundaries.

Benefiting from the improved perovskite film quality, the performance of the fabricated PSCs exhibit comparative or even improved PCE compared to the ones from traditional fabrication methods. More importantly, the feasibility of the organic gas assistant method for large scale PSCs fabrication is unparalleled. First, the quality of the raw perovskite film is not strictly required, which reduces the cost of perovskite film formation process. Second, the organic gas assistant method happens in very rapid period, shortens to seconds, which promotes the fabrication efficiency. Third, this gas treating method can eliminate the restriction of perovskite film area because of the uniformity of the fabricated films, which is compatible with the commercial printing technology.

Due to the burgeoning of the organic gas assistant method, there still remains some unexplored areas to be investigated in the future.

1. As mentioned above, the intermediate phase of $MAPbI_3 \cdot xMA$ is crucial for further understanding and optimization of MA gas based method. However, its instability restricts the sight into its essence and structure by traditional characterization methods. One possible way to solve this difficulty is to design specialized equipment, in which the atmosphere can hold the intermediate phase stable for in situ measurement. We hope more professional groups with different academic backgrounds can work together to make this important issue out.
2. Some works have been reported to fabricate large-scale PSCs in the laboratory by using MA gas or related methods. This indicates that by the combination of large-scale technologies (ink-jet printing, spray coating, slot-die printing, etc.) and MA gas healing method, industrialization of PSCs is extremely promising. The core technology of MA gas healing method needs to concern the precise control of the whole processing process to enable large-area raw films uniformly expose to MA gas and followed by a quick removal of the gas environment. The detailed parameters still need to be further optimized.
3. The pressure and concentration of the MA gas are varied in different works, and the treating duration is also not consistent. By regulating the gas pressure, concentration, degassing speed and even temperature, the crystallization process of perovskite grains is expected to be changed accordingly, which will affect the quality of the final perovskite films. Besides, the solvent of MA gas is another aspect which will influence the final film when using MA solution as the gas source, but the mechanism has not been in-depth studied. Generally, the dry MA gas is the best choice, followed by the MA gas in ethanol. MA gas in water is the worst because the MA gas molecules can combine the water

($MA \cdot H_2O$) and thus failed in healing the perovskite film. Therefore, to design specialized equipment which can exactly control the preparation parameters is very necessary.

4. The mixed perovskite system, including A site organic component mix (FA-MA, Cs-FA, Cs-MA-FA, etc.), B site metal component mix (Sn-Pb, Cu-Pb, etc.) and X site halogen component mix (I-Br, I-Cl, etc.) perovskites seems have their superior properties compared to traditional pure $MAPbI_3$ perovskite.[65–70] However their inherent different properties induced by their different mixed components make their gas-solid reaction dynamics complex. Therefore, the precise control of the organic gas method for mixed perovskite system still needs further investigation.
5. In addition to the application in PSCs, the application of organic gas-perovskite solid reaction has been reported in other fields such as perovskite light emitting diodes and subwavelength grating photonic application.[71–74] Due to the facile process and the magical properties transformation by the organic gas-perovskite solid reaction, it must have great potential to be extended to other applications in the future.

Acknowledgments

Financial support from the National Natural Science Foundation of China (51672290, 21671196, 61604156), the Youth Innovation Promotion Association of CAS (2015167), international S&T Cooperation Program of China (2015DFG62670), and the Qingdao Key Lab of Solar Energy Utilization and Energy Storage Technology are gratefully acknowledged. We thank Dr. Lioz Etgar of The Hebrew University of Jerusalem for his kind suggestions.

Keywords

large scale fabrication, methylamine gas, organolead halide perovskites, solar cells

Received: May 20, 2017
Revised: July 27, 2017
Published online: August 28, 2017

[1] A. Kojima, K. Teshima, Y. Shirai, T. Miyasaka, *J. Am. Chem. Soc.* **2009**, *131*, 6050.
[2] J. M. Frost, K. T. Butler, F. Brivio, C. H. Hendon, M. van Schilfgaarde, A. Walsh, *Nano Lett.* **2014**, *14*, 2584.
[3] G. E. Eperon, S. D. Stranks, C. Menelaou, M. B. Johnston, L. M. Herz, H. J. Snaith, *Energy Environ. Sci.* **2014**, *7*, 982.
[4] D. H. Cao, C. C. Stoumpos, O. K. Farha, J. T. Hupp, M. G. Kanatzidis, *J. Am. Chem. Soc.* **2015**, *137*, 7843.
[5] C. C. Stoumpos, C. D. Malliakas, M. G. Kanatzidis, *Inorg. Chem.* **2013**, *52*, 9019.
[6] H. Tsai, W. Nie, J. C. Blancon, C. C. Stoumpos, R. Asadpour, B. Harutyunyan, A. J. Neukirch, R. Verduzco, J. J. Crochet, S. Tretiak, L. Pedesseau, J. Even, M. A. Alam, G. Gupta, J. Lou, P. M. Ajayan, M. J. Bedzyk, M. G. Kanatzidis, *Nature* **2016**, *536*, 312.
[7] S. Pang, H. Hu, J. Zhang, S. Lv, Y. Yu, F. Wei, T. Qin, H. Xu, Z. Liu, G. Cui, *Chem. Mater.* **2014**, *26*, 1485.
[8] M. R. Filip, G. E. Eperon, H. J. Snaith, F. Giustino, *Nat. Commun.* **2014**, *5*, 5757.
[9] B. R. Sutherland, A. K. Johnston, A. H. Ip, J. Xu, V. Adinolfi, P. Kanjanaboos, E. H. Sargent, *ACS Photon.* **2015**, *2*, 1117.
[10] L. Zhang, T. Yang, L. Shen, Y. Fang, L. Dang, N. Zhou, X. Guo, Z. Hong, Y. Yang, H. Wu, J. Huang, Y. Liang, *Adv. Mater.* **2015**, *27*, 6496.
[11] D. B. Mitzi, *J. Mater. Chem.* **2004**, *14*, 2355.
[12] J. M. Azpiroz, E. Mosconi, J. Bisquert, F. De Angelis, *Energy Environ. Sci.* **2015**, *8*, 2118.
[13] H. D. Kim, H. Ohkita, *Solar RRL* **2017**, *1*, 1700027.
[14] Z. Xiao, W. Meng, J. Wang, D. B. Mitzi, Y. Yan, *Mater. Horiz.* **2017**, *4*, 206.
[15] Y. X. Zhao, K. Zhu, *J. Phys. Chem. Lett.* **2014**, *5*, 4175.
[16] N. J. Jeon, J. H. Noh, Y. C. Kim, W. S. Yang, S. Ryu, S. I. Seok, *Nature Mater.* **2014**, *13*, 897.
[17] M. Z. Liu, M. B. Johnston, H. J. Snaith, *Nature* **2013**, *501*, 395.
[18] L. Zuo, S. Dong, N. De Marco, Y. T. Hsieh, S. H. Bae, P. Sun, Y. Yang, *J. Am. Chem. Soc.* **2016**, *138*, 15710.
[19] K. K. Sears, M. Fievez, M. Gao, H. C. Weerasinghe, C. D. Easton, D. Vak, *Solar RRL* **2017**, *1*, 1700059.
[20] D. B. Khadka, Y. Shirai, M. Yanagida, T. Masuda, K. Miyano, *Sustain. Energy Fuels* **2017**, *1*, 755.
[21] Y. Zhou, K. Zhu, *ACS Energy Lett.* **2016**, *1*, 64.
[22] D. Vak, K. Hwang, A. Faulks, Y.-S. Jung, N. Clark, D.-Y. Kim, G. J. Wilson, S. E. Watkins, *Adv. Energy Mater.* **2015**, *5*, 1401539.
[23] T. M. Schmidt, T. T. Larsen-Olsen, J. E. Carlé, D. Angmo, F. C. Krebs, *Adv. Energy Mater.* **2015**, *5*, 1500569.
[24] Y. Hu, S. Si, A. Mei, Y. Rong, H. Liu, X. Li, H. Han, *Solar RRL* **2017**, *1*, 1600019.
[25] Z. Zhou, Z. Wang, Y. Zhou, S. Pang, D. Wang, H. Xu, Z. Liu, N. P. Padture, G. Cui, *Angew. Chem. Int. Ed.* **2015**, *54*, 9705.
[26] N. K. Noel, S. N. Habisreutinger, B. Wenger, M. T. Klug, M. T. Hörantner, M. B. Johnston, R. J. Nicholas, D. T. Moore, H. J. Snaith, *Energy Environ. Sci.* **2017**, *10*, 145.
[27] M. Long, T. Zhang, H. Zhu, G. Li, F. Wang, W. Guo, Y. Chai, W. Chen, Q. Li, K. S. Wong, J. Xu, K. Yan, *Nano Energy* **2017**, *33*, 485.
[28] S. R. Raga, L. K. Ono, Y. J. Qi, *Mater. Chem. A* **2016**, *4*, 2494.
[29] Y. Zhou, M. Yang, S. Pang, K. Zhu, N. P. Padture, *J. Am. Chem. Soc.* **2016**, *138*, 5535.
[30] Y. Zong, Y. Zhou, M. Ju, H. F. Garces, A. R. Krause, J. Fuxiang, G. Cui, X. C. Zeng, N. P. Padture, S. Pang, *Angew. Chem. Int. Ed.* **2016**, *55*, 14723.
[31] G. I. Gurina, K. V. Savchenko, *J. Photochem. Photobio. A: Chem.* **1993**, *86*, 81.
[32] N. Preda, L. Mihut, M. Baibarac, I. Baltog, R. Ramer, J. Pandele, C. Andronescu, V. Fruth, *J. Mater. Sci.: Mater. Electron.* **2008**, *20*, 465.
[33] B. Paloszt, W. Steurer, H. Schulz, *J. Phys.: Condens. Matter* **1990**, *2*, 5285.
[34] G. I. Gurina, K. V. Savchenko, *J. Solid State Chem.* **2004**, *177*, 909.
[35] V. Chakravarthy, A. M. Guloy, *Chem. Commun.* **1997**, *0*, 697.
[36] N. Preda, L. Mihut, I. Baltog, T. Velula, V. Teodorescu, *J. Optoelectron. Adv. Mater.* **2006**, *8*, 909.
[37] A. Ghorayeb, C. C. Coleman, A. D. Yoffe, *J. Phys. C: Solid State Phys.* **1984**, *17*, L715.
[38] R. Al-Jishi, C. C. Coleman, R. Treece, H. Goldwhite, *Phys. Rev. B* **1989**, *39*, 4862.
[39] G. Pellegrino, S. D'Angelo, I. Deretzis, G. G. Condorelli, E. Smecca, G. Malandrino, A. La Magna, A. Alberti, *J. Phys. Chem. C* **2016**, *120*, 19768.
[40] R. F. Warrent, W. Y. Liang, *J. Phys.: Condens. Matter* **1990**, *5*, 64074418.
[41] Y. Chang, L. Wang, J. Zhang, Z. Zhou, C. Li, B. Chen, L. Etgar, G. Cui, S. Pang, *J. Mater. Chem. A* **2017**, *5*, 4803.
[42] R. G. Niemann, A. G. Kontos, D. Palles, E. I. Kamitsos, A. Kaltzoglou, F. Brivio, P. Falaras, P. J. Cameron, *J. Phys. Chem. C* **2016**, *120*, 2509.

[43] T. Zhao, S. T. Williams, C. C. Chueh, D. W. deQuilettes, P. W. Liang, D. S. Ginger, A. K. Y. Jen, *RSC Adv.* **2016**, *6*, 27475.
[44] T. M. Brenner, Y. Rakita, Y. Orr, E. Klein, I. Feldman, M. Elbaum, D. Cahen, G. Hodes, *Chem. Mater.* **2016**, *28*, 6501.
[45] S. Ahmad, P. K. Kanaujia, W. Niu, J. J. Baumberg, G. Vijaya Prakash, *ACS Appl. Mater. Interfaces* **2014**, *6*, 10238.
[46] Z. Liu, J. Hu, H. Jiao, L. Li, G. Zheng, Y. Chen, Y. Huang, Q. Zhang, C. Shen, Q. Chen, H. Zhou, *Adv. Mater.* **2017**, *29*, 1606774.
[47] Y. Jiang, E. J. Juarez-Perez, Q. Ge, S. Wang, M. R. Leyden, L. K. Ono, S. R. Raga, J. Hu, Y. Qi, *Mater. Horiz.* **2016**, *3*, 548.
[48] T. Zhang, N. Guo, G. Li, X. Qian, L. Li, Y. Zhao, *J. Mater. Chem. A* **2016**, *4*, 3245.
[49] D. L. Jacobs, L. Zang, *Chem. Commun.* **2016**, *52*, 10743.
[50] B. Conings, S. A. Bretschneider, A. Babayigit, N. Gauquelin, I. Cardinaletti, J. Manca, J. Verbeeck, H. J. Snaith, H. G. Boyen, *ACS Appl. Mater. Interfaces* **2017**, *9*, 8092.
[51] M. Zhang, N. Wang, S. Pang, Q. Lv, C. Huang, Z. Zhou, F. Ji, *ACS Appl. Mater. Interfaces* **2016**, *8*, 31413.
[52] Y. Deng, E. Peng, Y. Shao, Z. Xiao, Q. Dong, J. Huang, *Energy Environ. Sci.* **2015**, *8*, 1544.
[53] Y. C. Zheng, S. Yang, X. Chen, Y. Chen, Y. Hou, H. G. Yang, *Chem. Mater.* **2015**, *27*, 5116.
[54] Y. Deng, Q. Dong, C. Bi, Y. Yuan, J. Huang, *Adv. Energy Mater.* **2016**, *6*, 1600372.
[55] T. Zhang, G. Li, F. Xu, Y. Wang, N. Guo, X. Qian, Y. Zhao, *Chem. Commun.* **2016**, *52*, 11080.
[56] D. Bi, W. Tress, M. I. Dar, P. Gao, J. Luo, C. Renevier, K. Schenk, A. Abate, F. Giordano, J. P. Correa Baena, J. D. Decoppet, S. M. Zakeeruddin, M. K. Nazeeruddin, M. Gratzel, A. Hagfeldt, *Sci. Adv* **2016**, *2*, e1501170.
[57] T. Zhang, N. Guo, G. Li, X. Qian, Y. Zhao, *Nano Energy* **2016**, *26*, 50.
[58] S. Pang, Y. Zhou, Z. Wang, M. Yang, A. R. Krause, Z. Zhou, K. Zhu, N. Padture, G. Cui, *J. Am. Chem. Soc.* **2016**, *138*, 750.
[59] W. Huang, J. S. Manser, S. Sadhu, P. V. Kamat, S. Ptasinska, *J. Phys. Chem. Lett.* **2016**, *7*, 5068.
[60] Y. Zhao, K. Zhu, *Chem. Commun.* **2014**, *50*, 1605.
[61] C. Bao, J. Yang, W. Zhu, X. Zhou, H. Gao, F. Li, G. Fu, T. Yu, Z. Zou, *Chem. Commun.* **2015**, *51*, 15426.
[62] S. Lv, S. Pang, Y. Zhou, N. P. Padture, H. Hu, L. Wang, X. Zhou, H. Zhu, L. Zhang, C. Huang, G. Cui, *Phys. Chem. Chem. Phys.* **2014**, *16*, 19206.
[63] M. Long, T. Zhang, Y. Chai, C. F. Ng, T. C. Mak, J. Xu, K. Yan, *Nat. Commun.* **2016**, *7*, 13503.
[64] C. Li, Z. Wang, Y. Chang, Y. Zong, F. Ji, B. Zhang, H. Li, S. Pang, *RSC Adv.* **2016**, *6*, 85026.
[65] M. Saliba, T. Matsui, J.-Y. Seo, K. Domanski, J.-P. Correa-Baena, M. K. Nazeeruddin, S. M. Zakeeruddin, W. Tress, A. Abate, A. Hagfeldt, M. Grätzel, *Energy Environ. Sci.* **2016**, *9*.
[66] D. P. McMeekin, G. Sadoughi, W. Rehman, G. E. Eperon, M. Saliba, M. T. Hoerantner, A. Haghighirad, N. Sakai, L. Korte, B. Rech, M. B. Johnston, L. M. Herz, H. J. Snaith, *Science* **2016**, *351*, 151.
[67] N. J. Jeon, J. H. Noh, W. S. Yang, Y. C. Kim, S. Ryu, J. Seo, S. I. Seok, *Nature* **2015**, *517*, 476.
[68] D. Zhao, Y. Yu, C. Wang, W. Liao, N. Shrestha, C. R. Grice, A. J. Cimaroli, L. Guan, R. J. Ellingson, K. Zhu, X. Zhao, R.-G. Xiong, Y. Yan, *Nature Energy* **2017**, *2*, 17018.
[69] D. Cortecchia, H. A. Dewi, J. Yin, A. Bruno, S. Chen, T. Baikie, P. P. Boix, M. Gratzel, S. Mhaisalkar, C. Soci, N. Mathews, *Inorg. Chem.* **2016**, *55*, 1044.
[70] L. A. Frolova, D. V. Anokhin, K. L. Gerasimov, N. N. Dremova, P. A. Troshin, *J. Phys. Chem. Lett.* **2016**, *7*, 4353.
[71] M. S. Alias, Y. Yang, T. K. Ng, I. Dursun, D. Shi, M. I. Saidaminov, D. Priante, O. M. Bakr, B. S. Ooi, *J. Phys. Chem. Lett.* **2016**, *7*, 137.
[72] S. D. Stranks, H. J. Snaith, *Nat. Nanotech.* **2015**, *10*, 391.
[73] H. Zhu, Y. Fu, F. Meng, X. Wu, Z. Gong, Q. Ding, M. V. Gustafsson, M. T. Trinh, S. Jin, X. Y. Zhu, *Nature Mater.* **2015**, *14*, 636.
[74] M. I. Saidaminov, V. Adinolfi, R. Comin, A. L. Abdelhady, W. Peng, I. Dursun, M. Yuan, S. Hoogland, E. H. Sargent, O. M. Bakr, *Nat. Commun.* **2015**, *6*, 8724.